Supporting Information

Liu et al. 10.1073/pnas.1618307114

SI Text

Materials. The hydrogel was composed of two types of cross-linked polymers: ionically cross-linked alginate and covalently cross-linked PAAm. For the stretchy PAAm network in hydrogel, acrylamide (AAm; A8887; Sigma-Aldrich) was used as the monomer, *N*,*N*-methylenebisacrylamide (MBAA; 146072; Sigma-Aldrich) was used as the cross-linker, and 2-hydroxy-4′-(2-hydroxyethoxy)-2-methylpropiophenone (Irgacure 2959; 410896; Sigma-Aldrich) was used as the photoinitiator. Calcium sulfate (C3771; Sigma-Aldrich) slurry acted as the ionic cross-linker with sodium alginate (A2033; Sigma-Aldrich) for the dissipative network. As for elastomers, Sylgard 184 [polydimethylsiloxane (PDMS; Dow Corning] or Ecoflex (Smooth-On) was molded and activated with benzophenone (B9300; Sigma-Aldrich). Purple Nitrile Examination Gloves (Kimberly-Clark) were also used as an elastomer substrate. Ammonium persulfate (APS; A3678; Sigma-Aldrich) as a thermoinitiator and *N*,*N*,*N*′,*N*′-tetramethylethylenediamine (TEMED; T9281; Sigma-Aldrich) as a cross-linking accelerator were used in the fast-curable pregel solution for sealing of injection points. For cell induction, DAPG (sc-206518; Santa Cruz Biotechnology), AHL (K3007; Sigma-Aldrich), IPTG (I5502; Sigma-Aldrich), Rham (W373011; Sigma-Aldrich), and aTc (37919; Sigma-Aldrich) were used as the signaling molecules. Carbenicillin (C1389; Sigma-Aldrich) was added as an antibiotic in the LB–Miller medium (L3522; Sigma-Aldrich) for cell culture. The LIVE/DEAD BacLight Bacterial Viability and Counting Kit (L34856; Sigma-Aldrich) was used for cell viability assay.

Fabrication of Hydrogel and Elastomer Hybrid. Elastomers with microstructured cavities were prepared by soft lithography with the feature size of 500 μm in width and 200 μm in depth. Then, the prepared microstructured elastomer was assembled with hydrogel to form robust hydrogel–elastomer hybrid as described in the previous report (15). Briefly, the surface of the elastomer was treated with 10% (wt/vol) benzophenone solution in ethanol for 10 min, washed, and dried with nitrogen. The pregel solution [12.05% (wt/vol) AAm, 1.95% (wt/vol) sodium alginate, 0.2% Irgacure 2959, 0.012% MBAA] was carefully degassed and mixed with calcium sulfate slurry (2×10^{-2} M in pregel solution) to form physically cross-linked hydrogel. To introduce robust bonding between assembled hydrogel and elastomer, the physically cross-linked hydrogel was assembled with the surface treated elastomer followed by UV irradiation (365 nm; UVP CL-1000) for 30 min. The resultant hydrogel–elastomer hybrid was washed with PBS for three times, sterilized using germicidal UV irradiation thoroughly, and immersed in LB with antibiotics for 12 h before bacterial cell seeding. Fast-curable pregel solution [30.05% (wt/vol) AAm, 1.95% (wt/vol) sodium alginate, 0.012% MBAA, 0.142% APS, 0.10% TEMED], which could be cured at room temperature in 5 min, is used for sealing the holes after cell seeding.

Bacterial Strains and Plasmids. The plasmids used in this study were constructed with standard molecular cloning techniques. To create constructs for the expression of output genes under tight regulation by DAPG-, IPTG-, AHL-, or Rham-inducible promoters, pZE-AmpR-pL(lacO)-*gfp* (IPTG-inducible) was used as a starting point. All promoters were amplified using PCR and inserted in place of pL(LacO) by Gibson assembly. The corresponding repressors or activators, which can interact with small molecule inducers, were inserted into the *Escherichia coli* genome or cloned onto the same plasmid that harbors the promoter-*gfp* output module. For example, the proteins PhlF and LacI repressed DAPG- and IPTG-inducible promoters, respectively. PhlF was inserted in a plasmid under regulation of proD promoter, whereas the LacI repressor was already present in the genome of DH5αPRO. Similarly, the AHL-inducible transcriptional activator, LuxR, was constitutively expressed from a plasmid and can activate promoter pLuxR on binding to AHL. The regulatory components necessary for Rham induction were already present in the *E. coli* genome and did not required additional engineering. To construct the AHL sender plasmid, *LuxI* was put onto a plasmid under the regulation of aTc-inducible promoter PLtetO. Finally, all ligations for plasmid construction were transformed into *E. coli* strain DH5αPRO with standard protocols and are described in Fig. S6.

Cell Induction in the Living Device. The cell-contained device was immersed in LB broth with carbenicillin and inducer(s) at 25 °C as mentioned in the text. Inducers could be added in LB at final concentrations of 100 μM DAPG, 100 nM AHL, 1 mM IPTG, 12 mM Rham, and/or 200 ng/mL aTc. Alternatively, a piece of sterilized tissue paper (Kimtech) was dipped in LB with inducer in it and put on top of the hydrogel layer. The device and the tissue paper were kept at 25 °C and relative humidity of 90%. The latter method was not only applicable for the cell to receive inducers from the environment (e.g., induction of $IPTG_{RCV}$/GFP by IPTG) but also, more suitable for intercellular communication when dilution of signaling molecules by the environment was undesirable. Every induction/detection experiment was performed and repeated at least three times.

Cell Viability Assay. By using the LIVE/DEAD BacLight Bacterial Viability and Counting Kit in combination with flow cytometry, the cell viability assay was conducted for cells retrieved from devices and live/dead controls. The fluorescent LIVE/DEAD BacLight Bacterial Viability and Counting Kit consists of two stains: the green fluorescent nucleic acid stain SYTO 9, which stains the nucleic acids of both living and dead bacteria, and the red fluorescent nucleic acid stain propidium iodide, which only stains bacteria that have damaged and leaky membranes. $Rham_{RCV}$/GFP bacterial suspensions were retrieved from the device by poking a hole from the hydrogel using metal needles after 12, 24, 48, and 72 h of culturing. Live-cell controls (untreated) and dead-cell controls (isopropyl alcohol-treated) were set as standards. A diluted bacterial suspension and the LIVE/DEAD BacLight solution were mixed together and incubated at room temperature protected from light for 15 min. The stained cell samples were then analyzed by an LSRFortessa Flow Cytometer (BD Biosciences). For each sample, at least 10^4 events were recorded using a flow rate of 0.5 μL/s. FlowJo (TreeStar) was used to analyze the data. All events were gated by forward scatter and side scatter. In Fig. S2, green fluorescence denotes both live and dead bacteria, and the red fluorescence denotes bacteria that have been damaged and leaky membranes. The distributions of the live and dead populations were distinguished in the cytograms.

Cell Escape Test. An intact hydrogel–elastomer living device, and a defective living device (with weak hydrogel–elastomer bonding) were tested for comparison. Also, the agar hydrogel with the same dimensions as the hydrogel–elastomer hybrid and encapsulating $Rham_{RCV}$/GFP bacteria was used as a control. We first deformed the living materials, which contained $Rham_{RCV}$/GFP bacteria in different modes (i.e., twisting and stretching), and then, immersed them in LB for 24 h. To test the bacteria leakage, LB solutions

surrounding the device were collected for streaking on LB agar plates after 24 h, and OD_{600} measurements by UV-Visible Spectrophotometer (Thermo Scientific) were taken after 6, 12, 20, and 24 h.

In addition, we prepared agar hydrogel with bacteria encapsulated: 1.5% (wt/vol) agar was dissolved in water at 90 °C. When the agar solution cooled down to ~40 °C, the $Rham_{RCV}$/GFP bacteria was mixed with the solution. As it continued to cool down, the solution could solidify and became a gel.

GFP Expression Assay. For quantitative measurement of GFP expression, the bacteria were isolated from the device by 32-gauge needles and diluted to 10^7 cells per 1 mL. Single-cell fluorescence was measured using an LSRFortessa Flow Cytometer with a 488-nm laser for GFP. For each sample, at least 10^4 events were recorded using a flow rate of 0.5 μL/s. FlowJo was used to analyze the data. All events were gated by forward scatter and side scatter. Integration of cell numbers over fluorescence was calculated and normalized to the maximum fluorescence. For qualitative observation of GFP expression by the naked eye, the living devices were exposed to benchtop UltraSlim Blue Light Transilluminators (New England Biogroup; wavelength of 470 nm). We extracted the green channel from optical images and adjusted the exposure by setting gamma correction to 0.2 in Adobe Photoshop CS6 (Adobe). Microscopic observation was done by the aid of a fluorescent microscope (Nikon Eclipse LV100ND), and all imaging conditions, such as beam power and exposure time, were maintained the same across different samples.

Preparation and Testing of Sensor Patch on Skin. The robust hybrid patches with wavy microchannels were fabricated by using hydrogel (PAAm-alginate) and silicone elastomer (Sylgard 184) following the previously described method. Bacterial suspension of $Rham_{RCV}$/GFP was infused to the upper two channels of the patch, and AHL_{RCV}/GFP was infused to the lower two channels of the patch. Before we adhered the living patch on forearm, the skin was smeared with LB of 12 mM Rham and/or 100 nM AHL. Note that these two inducers are nontoxic and safe to be applied on skin. The living patch was conformably mounted on the skin with the PDMS layer exposed to air and fixed on the skin by a clear Scotch tape. To show the antidehydration property of the wearable living patch, a pure hydrogel device without elastomer layer was fabricated by assembling micropatterned hydrogel and flat hydrogel sheet. To compare dehydration of hydrogel–elastomer hybrids and the hydrogel device without the elastomer layer, these two types of devices were conformably attached to curved surfaces of plastic beakers. The dehydration tests were carried out at room temperature with low humidity (25 °C and 50% relative humidity) for 24 h. To show the stretchability of living patch, we also fabricated the living skin patch with Ecoflex instead of PDMS in the same design and dimension. As illustrated in Fig. S3, the stretchable skin patch with induced bacteria can be stretched and relaxed to 1.8 times its original length without failure.

Preparation and Testing of Living Chemical Detectors on Nitrile Glove Fingertips. To show the living chemical sensors at the nitrile glove fingertips, hydrogel–elastomeric glove hybrids with spiral microchannels were prepared. We first laminated thin hydrogel sheets with patterned cell chambers on the fingertips of nitrile gloves and then, encapsulated different inducible cell inside. Different strains of bacteria ($IPTG_{RCV}$/GFP, AHL_{RCV}/GFP, and $Rham_{RCV}$/GFP) were injected into spiral-shaped cell chambers at different fingertips. To test the functionality of the fingertip sensor array, we used a cluster of cotton balls soaked in LB with 1 mM IPTG and 12 mM Rham. The glove was worn to grab the wet cotton balls, and hydrogels at the fingertips contacted the inducer-containing cotton balls. The fluorescence at the fingertips was exampled after 4 h of contact with the cotton balls using the benchtop transilluminator.

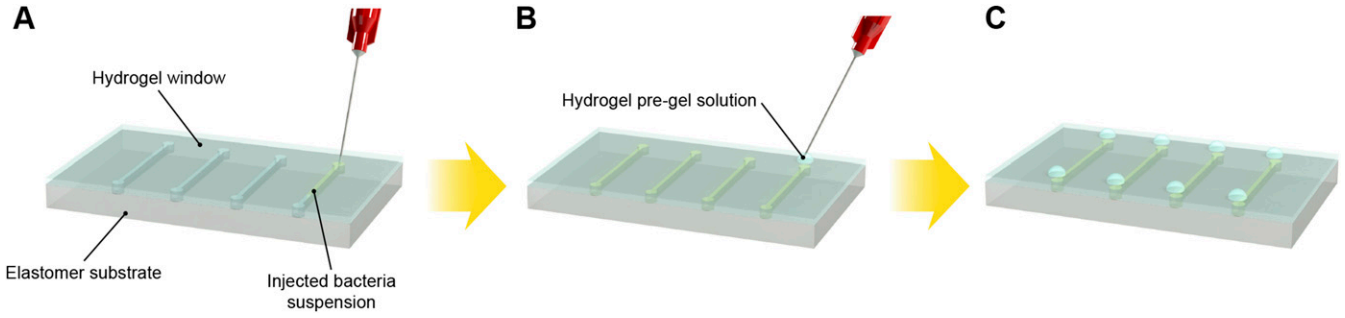

Fig. S1. Schematic illustration of cell suspension injection and sealing of injection points. (*A*) Bacteria were injected into the cavities at the hydrogel–elastomer interface with metallic needles from the hydrogel side. (*B*) Injection holes were sealed on the hydrogel–elastomer device with drops of fast-curable pregel solution. (*C*) We obtained the hydrogel–elastomer device with fully encapsulate bacteria.

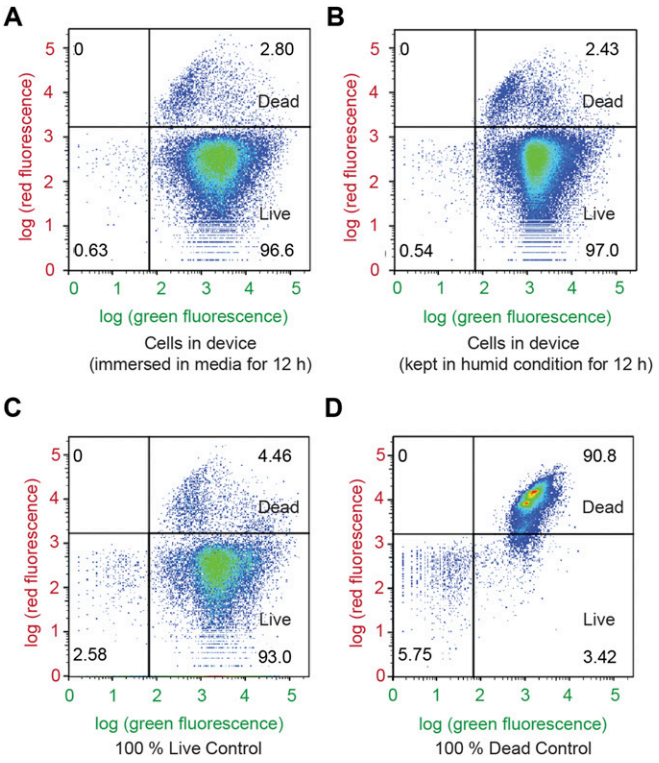

Fig. S2. Flow cytometry analysis using live/dead stains for (*A*) cells retrieved from the living device that has been immersed in media for 12 h, (*B*) cells retrieved from the living device that has been placed in humid environment for 12 h, (*C*) live-cell controls, and (*D*) dead-cell controls. Green fluorescence denotes both live and dead bacteria, and red fluorescence denotes bacteria that have been damaged and leaky membranes. The distributions of the live and dead populations are illustrated in the plots, with thresholds determined by controls. Over 95% of cells in the hydrogel–elastomer devices immersed in media or placed in humid chamber remained viable after 12 h.

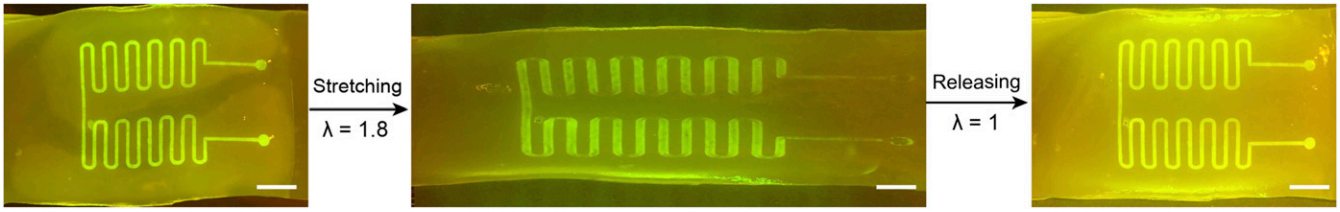

Fig. S3. Functional living device under large uniaxial stretch. After GFP was switched on in the wavy channels of Ecoflex–hydrogel hybrid matrix, the device was stretched to 1.8 times its original length and then released. The device, including cells encapsulated, can maintain functionality under large deformation without failure or leakage. (Scale bar: 5 mm.)

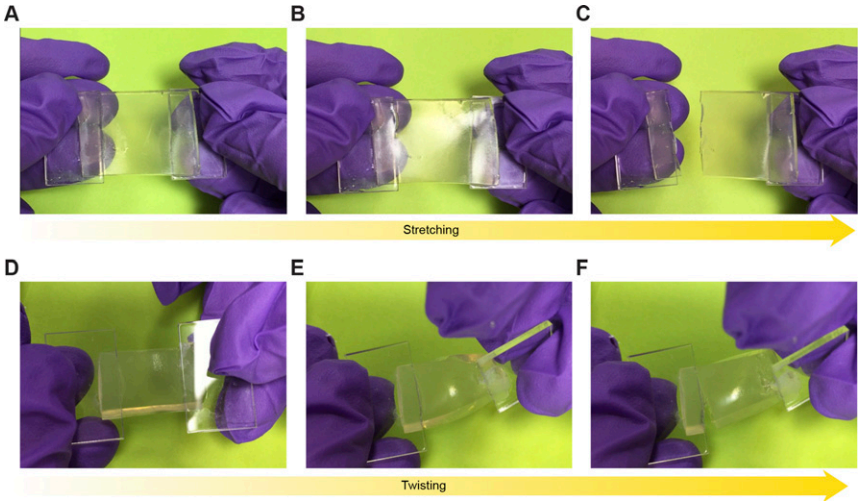

Fig. S4. Deformation of agar-based living devices. An agar-based control device that encapsulated $Rham_{RCV}$/GFP bacteria with the same dimensions as the hydrogel–elastomer hybrid was fabricated. The agar device fractured even under moderate deformation, including (*A*–*C*) a stretch of 1.1 or (*D*–*F*) a twist of 60°.

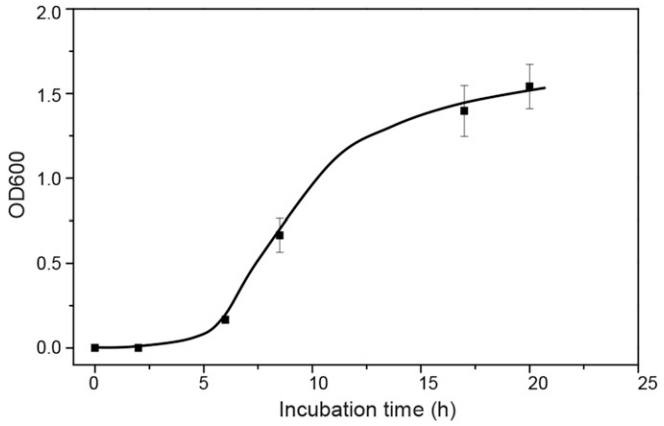

Fig. S5. Cell leakage from the agar device. The medium surrounding the agar device (without any deformation) was collected to measure OD_{600}. The high OD_{600} after 10 h indicates the large cell populations in the medium and cell leakage even without any deformation of agar gel.

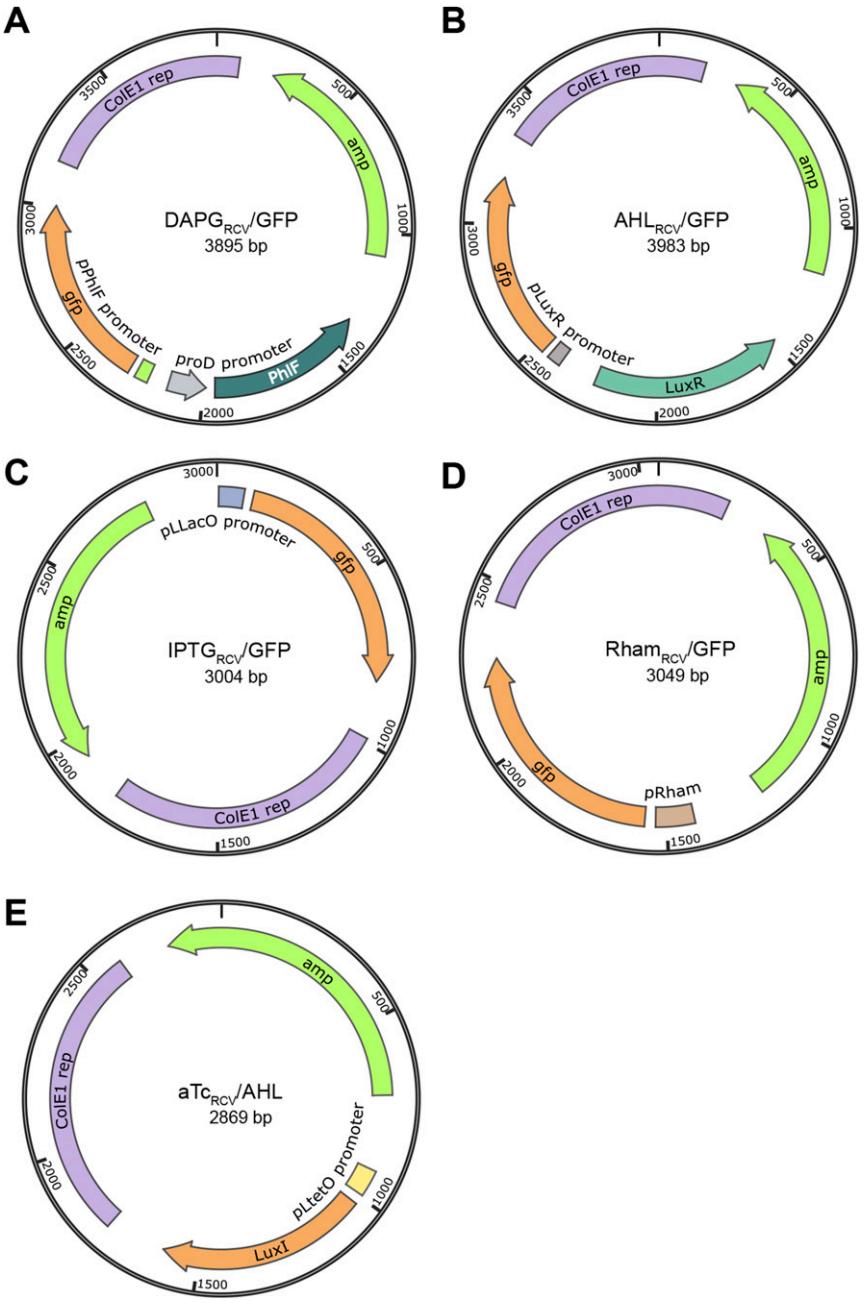

Fig. S6. Plasmid maps of the plasmids constructed. (*A*) DAPG$_{RCV}$/GFP, (*B*) AHL$_{RCV}$/GFP, (*C*) IPTG$_{RCV}$/GFP, (*D*) Rham$_{RCV}$/GFP, and (*E*) aTc$_{RCV}$/AHL. Plasmids were constructed as described in *SI Text*. amp, Ampicillin resistance gene; ColE1 rep:, replication origin from ColE1 plasmid.

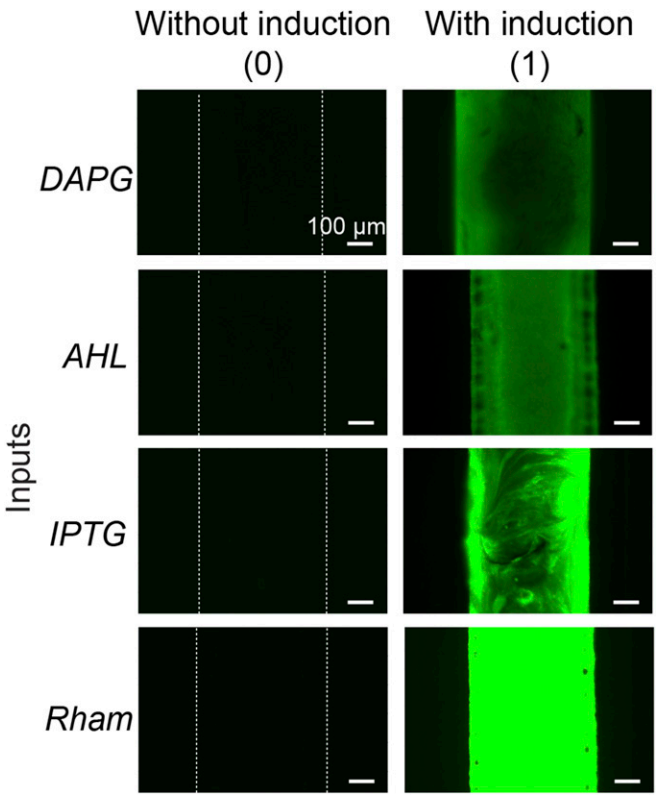

Fig. S7. Microscopic images of different cell strains in the chamber encapsulated in the living device. When a cell strain was induced, the channels showed fluorescence [denoted as (1)]. If not induced, the channel stayed dark [denoted as (0)]. Scale bars are shown in images.

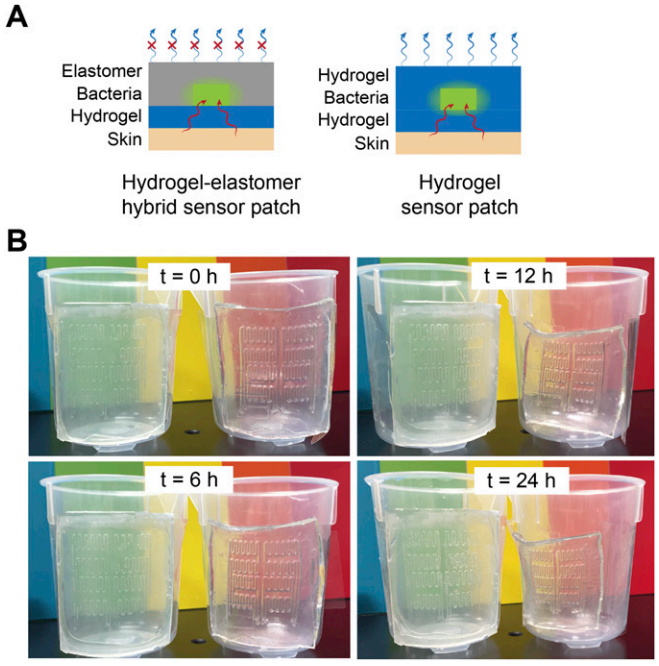

Fig. S8. Antidehydration property of the sensor patch. (*A*) Schematic illustration of the hydrogel–elastomer hybrid sensor patch, which has the antidehydration property over the pure hydrogel device. The silicone elastomer cover effectively prevents evaporation of water from the hydrogel and dehydration of the living patch. (*B*) Time-lapse snapshots of hydrogel–elastomer hybrid sensor patch (*Left*) and pure hydrogel sensor patch (*Right*) mounted on a plastic beaker at room temperature with low humidity (25 °C and 50% relative humidity) for 24 h. The elastomer outer layer of the hydrogel–elastomer hybrid device significantly slowed down the dehydration process of the hydrogel and provided a sustained humid environment for encapsulated cells for over 24 h. However, distorted channels became apparent on patches made of pure hydrogels when they were exposed to air for 6 h because of dehydration.

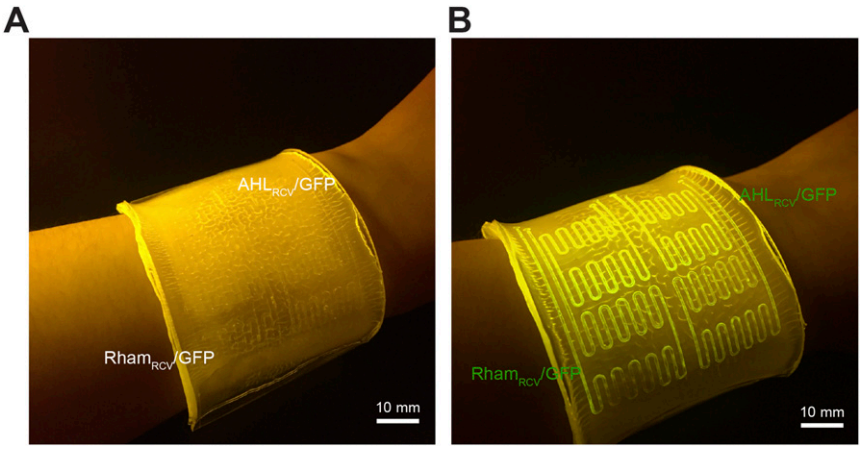

Fig. S9. Living patch control experiments. (*A*) When no inducer was smeared on skin and the living sensor patch was adhered on skin conformably, the channels with Rham$_{RCV}$/GFP and AHL$_{RCV}$/GFP in the living patch did not show any differences. (*B*) When both inducers Rham and AHL were smeared on skin and the living patch was applied, the channels with Rham$_{RCV}$/GFP and AHL$_{RCV}$/GFP in the living patch became fluorescent. Scale bars are shown in images.

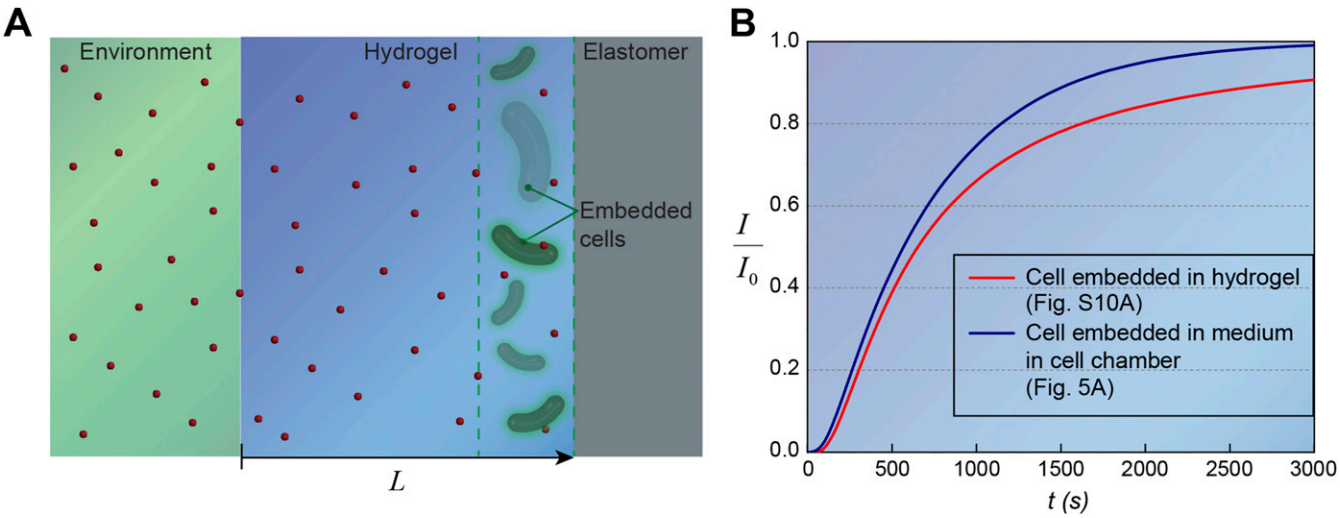

Fig. S10. Calculation of critical diffusion timescales for living materials and devices. (*A*) Schematic illustration of signaling molecule diffusion from the environment through the hydrogel in the living device. Cells were embedded in a segment of the hydrogel close to the elastomer wall. (*B*) Comparison of typical inducer concentration profiles when cells were embedded in hydrogel $[I(L, t)/I_0]$ vs. cells in medium of the cell chamber $[I(L_g + L_c/2, t)/I_0]$. Despite small deviation (<12%) because of the diffusivity differences between hydrogel and medium and distance variation in two cases, it can be seen that the profile in the simplified model can consistently represent the typical concentration profile in the cell chamber of the living sensor at any time.

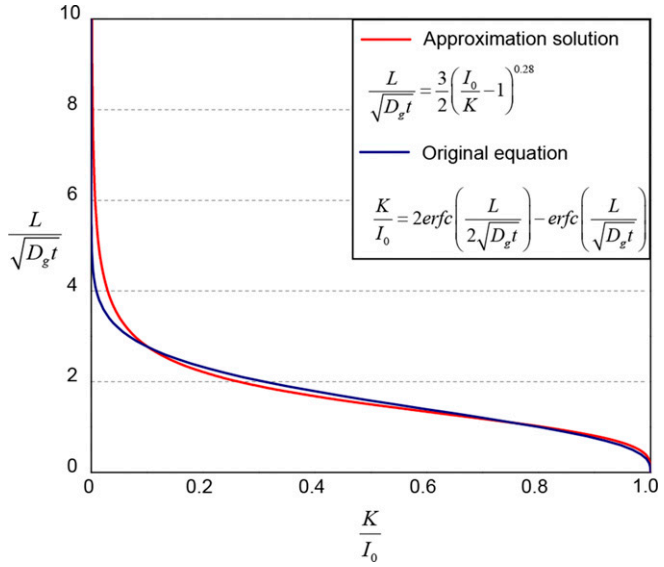

Fig. S11. Approximate diffusion timescale. The expression of $K/I_0 = 2erfc[L/2\sqrt{D_g t}] - erfc[L/\sqrt{D_g t}]$ and its approximate solution. The prefactor in $t_{diffuse} = [\Lambda(K/I_0)]^{-2} L^2/D_g$ is fitted into a power law that approximately gives $t_{diffuse} \approx 4/9(I_0/K - 1)^{-0.56} L^2/D_g$.